Applied Thermal Engineering 108 (2016) 20–29

Contents lists available at ScienceDirect

Applied Thermal Engineering

journal homepage: www.elsevier.com/locate/apthermeng

Research Paper

Temperatures in shallow marine sediments: Influence of thermal properties, seasonal forcing, and man-made heat sources

Christian Müller *, Regina Usbeck, Frederieke Miesner

FIELAX Gesellschaft für wissenschaftliche Datenverarbeitung mbH, Schleusenstr. 14, 27568 Bremerhaven, Germany

HIGHLIGHTS

- Sediment thermal properties are highly variable.
- Seasonal forcing causes large spatial and temporal sediment temperature variations.
- Power cable temperatures strongly depend on thermal properties of a given site.
- The 2 K-criterion is not suitable to detect man-made heat injection.

ARTICLE INFO

Article history:
Received 20 April 2016
Revised 4 July 2016
Accepted 16 July 2016
Available online 17 July 2016

Keywords:
Offshore power cable temperature
Sediment thermal properties
Marine heat flux
2 K-criterion

ABSTRACT

Analytical and 2D finite-element solutions of the heat transfer equation are used to model the temperature evolution in the upper 15 m of marine sediment deposits. These calculations comprise realistic, in-situ measured, thermal properties as well as natural (geothermal and sea bottom temperature) and man-made (e.g. high voltage, subsea power cables) heat sources. A main objective of this article is to focus on the influence of the thermal heterogeneity of sediments in the North and Baltic Seas. In combination with seasonal variations of bottom water temperatures, these result in large temperature differences in the upper 3–5 m of the sediments. Also, the impact of additional heat through power cables is considered. The modelling results show maximum cable temperatures as much as 16 K difference less compared to a conservative homogeneous scenario previously used from literature values. It can be shown that the *2 K-criterion* is not a suitable instrument to monitor the man-made impact to the thermal conditions without knowing the actual thermal settings of a given location.

1. Introduction

Offshore wind farms have an enormous potential of replacing conventional energy sources. These wind farms are connected to the shore by high voltage power cables crossing distances of more than 100 km in the marine environment. The cables are usually buried within the sediments. Depending on the power transmission, the cables produce more or less dissipative heat, which is released into the sediments. This process leads to two effects: cooling of the cable and heating of the surrounding sediments. The operators of the power cables are interested in both processes: A 'cool' cable is more effective for power transmission whereas heating of the sediments is important because of a possible negative influence on benthic biological communities.

In the German exclusive economic zone (EEZ), the environmental impact of a cable installation is to be limited according to the principal legal stipulations authorized by the Bundesamt für Seeschifffahrt und Hydrographie (BSH) [1]. A major concern is that the temperature conditions for benthic life-forms shall be held at 'natural' levels. Therefore, the 2 K-criterion was proposed by the Bundesamt für Naturschutz (BfN) [2]. The 2 K-criterion stipulates that the maximum allowable temperature rise at 0.2 m sediment depth, vertical above a power cable, shall not exceed 2 K compared to undisturbed conditions.

Offshore energy cables are designed for maximum core temperatures of about 90 °C and sheath temperatures of up to 60 °C during full load events. Obviously, an amount of thermal energy is injected to the surrounding sediments. In order to estimate the temperatures in the surrounding sediments, an understanding of the thermal properties of the sediments, natural temperature levels, and their variability is essential.

Analytical and finite element models are used to calculate the natural temperature distribution. The models incorporate the geothermal heat flow as well as temperature variations through seasonal variations of the bottom water temperature. The input

* Corresponding author.
E-mail address: mueller@fielax.de (C. Müller).

http://dx.doi.org/10.1016/j.applthermaleng.2016.07.105
1359-4311/

parameters used in the models are measured thermal properties and bottom-water temperatures as published by the BSH [3]. A superimposition of the (time-dependent) additional heat caused by power cables is then used to predict resulting temperature distributions for full seasonal/annual cycles. A comparison of model results for a given configuration of cable properties and burial depth with/without additional heat through a full annual cycle allows a good understanding of the influence on the temperature distribution in the sediments. An evaluation of temperature changes at cable burial depth and in 0.2 m sub-bottom depth, shows the cooling effects on the cable as well as a possible violation of the 2 K-criterion.

International standards (IEC and IEEE) for calculation of the thermal resistance between power cables and the surrounding environment are based on analytic considerations of Nether and McGrath from 1957 [4]. Until recently, numerous scientific works dealing with the thermal regime around buried power cables have been published. These include finite-element simulations in heterogeneous multi-layered sediments [e.g. 5–9], also including effects of trench backfill material [10] as well as the influence of convective water transport in permeable sediments [11,12]. A considerable problem is the knowledge about the true thermal properties of the sediments. To overcome this, other authors [13,14] used results from laboratory experiments as a foundation for finite-element computational models. As a different approach, we use direct in-situ thermal properties measurements combined with natural, realistic temperature variations of the sediments as an input for analytical and finite-element modelling.

2. Measurement of temperatures and sediment thermal properties

2.1. The VibroHeat method

In principle, the sediment thermal properties can be measured either in-situ or by using sediment core samples [15]. The data used in this study have been gained using the 'VibroHeat' method. The principle for the measurements of depth dependent thermal parameters originates from the classical method of determining steady-state heat flow values for the oceanic crust from soft deep-sea sediments using heat flow probes penetrating by their own weight [16]. However, sediments in the North and Baltic Seas have higher shearing resistance. For successful penetration, a thermistor string has been combined with a standard VKG vibrocorer [17]. As for the problem addressed, the upper 3–4 m of the sediments are of major interest, and a system was used which allows the in-situ measurement of temperatures and thermal parameters from 22 thermistors at a vertical resolution of 13.5 cm down to a depth of 3.5 m. Sediment thermal conductivities are determined from the decay of a defined, artificial heat pulse. With these data, the natural, undisturbed vertical variability of sediment temperatures and thermal properties can be obtained. The measuring procedure follows the classical approach. The system is lowered towards the sediment, penetrates, and rests in the sediment for in-situ temperature measurement and heat pulse decay recording. Fig. 1 shows the measurement principle.

2.2. Determination of thermal parameters

The determination of in-situ temperatures and thermal material properties is based on an inversion algorithm following the work of Hartmann and Villinger [18]. Based on the assumption of the thermal decay around a cylindrical, symmetric, infinite line source, steady state in-situ temperatures (T), thermal conductivities (λ) and thermal diffusivities (κ) are determined in an iterative procedure. It should be kept in mind that layered sediment deposits are transversely isotropic and therefore exhibit a conductivity anisotropy showing larger conductivities in horizontal than in vertical direction. Following Pribnow et al. [19], this anisotropy is $\lambda_{horizontal}/\lambda_{vertical} \sim 1.2$. From thermal conductivities and diffusivities also the volumetric thermal capacities can be determined by $\rho c_v = \lambda/\kappa$, where ρ is the density of the sediment and c_v the heat

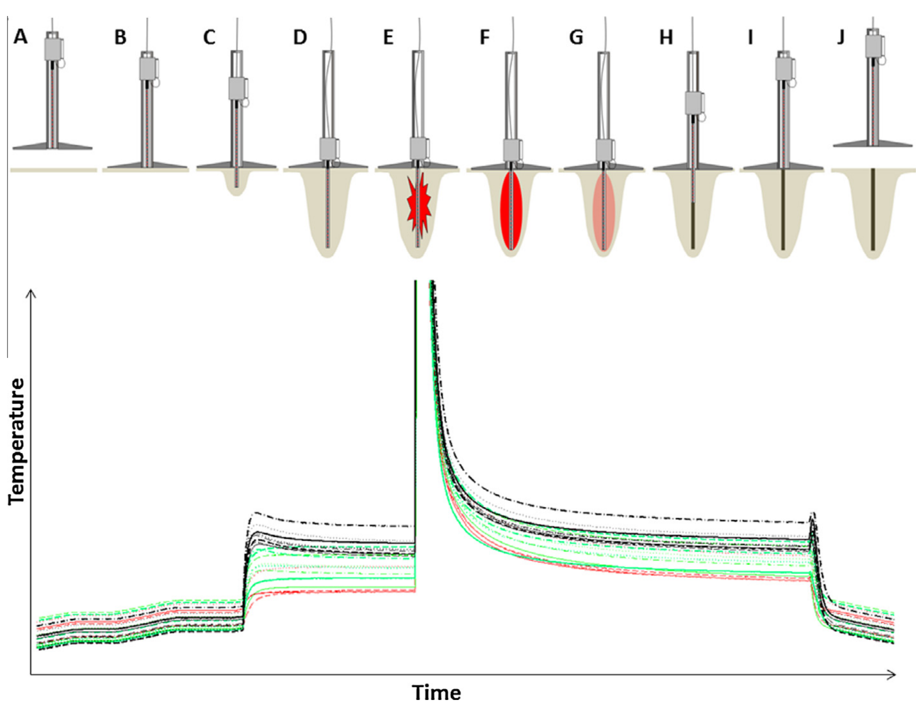

Fig. 1. Principle of a thermal parameters measurement used in combination with a vibrocorer: A-B: VibroHeat lowering to the seabed. C: Penetrating into seabed. D: Recording temperatures of thermal decay of frictional heat for the determination of undisturbed sediment temperatures. E: Artificial heat pulse. F-I: Recording temperatures of thermal decay of heat pulse for determination of thermal conductivities and diffusivities. J: Pullout and retrieval to surface. The lower panel shows the corresponding temperature recordings of the 22 thermistors.

capacity. The relative errors for thermal diffusivity, which is the input for modelling, are typically <10% as derived from the inversion scheme [18]. Nevertheless, thermal conductivity errors are significantly smaller and a valuable control for the reliability of the measurements is provided by typical stable values within 2.5–3.0 MJ m^{-3} K^{-1} for the volumetric thermal capacities.

Depth-dependent properties from measurements performed in the Baltic Sea in June 2011 from three different sites (Fig. 2a-c) indicate high spatial variability. At all locations, contrary to the general positive temperature gradient in the Earth's crust, the temperatures decrease with increasing depth. This is due to the seasonal variation of the bottom-water temperature in the Baltic

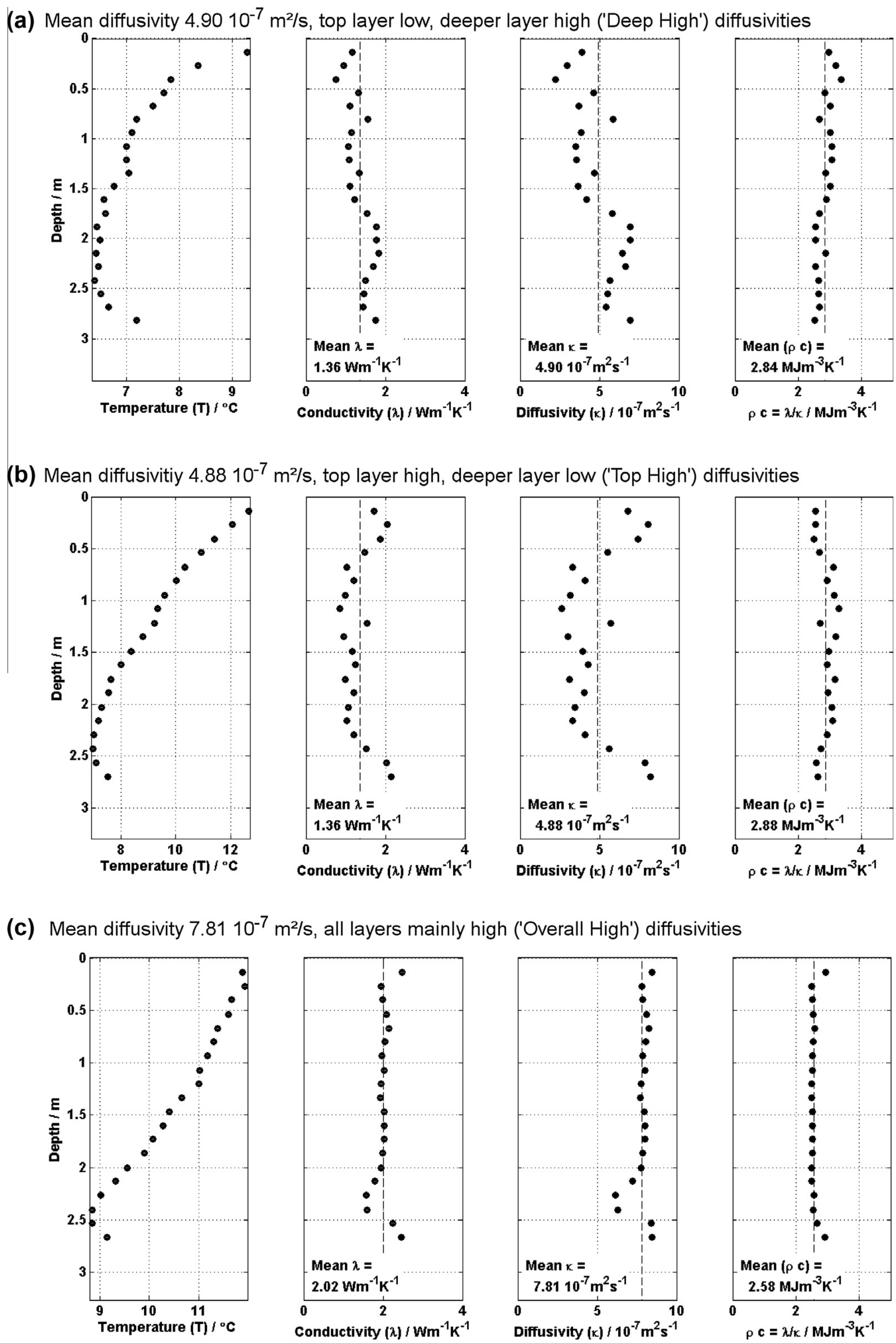

Fig. 2. Thermal parameters as measured at three sites in the Baltic Sea showing depth-dependent temperatures, thermal conductivities, diffusivities, and capacities. Conductivities and diffusivities are quite heterogeneous with depth showing specifically **(a)** low values in the upper first metre, **(b)** high values in the upper 0.5 m and low below, and **(c)** overall high values. A valuable control for the reliability of the measurements is the volumetric capacity (ρc_v) with typical stable values of 2.5–3.0 MJ m^{-3} K^{-1} for marine sediments.

Sea, as the measurements were performed in June, i.e. the influence of the warm summer temperatures is seen in the upper thermistors. The decreasing temperatures towards the deeper regions are relics of cold winter temperatures. As can be seen, the temperature distribution with depth differs at the three stations, which already indicates that the thermal parameters of these sediments must be different as the prevailing bottom water temperatures are about the same.

The parameters determined for each site include the corresponding depth-dependent thermal conductivity, temperature diffusivity, and volumetric thermal capacity (Fig. 2). The first example (**a**) shows higher thermal diffusivities in the deeper layers and lower values above, whereas the second (**b**) features higher diffusivities in the upper layers and lower values below. The mean thermal diffusivities are similar ($4.90 \cdot 10^{-7}\,m^2/s$ resp. $4.88 \cdot 10^{-7}\,m^2/s$). The last example (**c**) shows smooth varying thermal conductivities and diffusivities on relatively high levels. In the following, for brevity the profiles have been named (**a**) 'Deep High', (**b**) 'Top High', and (**c**) 'Overall High'.

3. Modelling of sediment temperature distributions

For modelling the thermal energy release of a buried power cable and accompanied temperature field evolution ($T(\vec{r},t)$) in the marine sediment, the heat transfer equation with an internal source term described by the heat source density $H(\vec{r},t)$ at point $\vec{r}$ and time t is solved:

$$\rho(\vec{r})c_v(\vec{r})\partial_t T(\vec{r},t) - \nabla\cdot(\lambda(\vec{r})\nabla T(\vec{r},t)) = H(\vec{r},t) \quad (1)$$

With assumed volumetric heat capacities $\rho(\vec{r})c_v(\vec{r}) = \lambda/\kappa = const$ (λ thermal conductivity and κ thermal diffusivity) this simplifies to

$$\partial_t T(\vec{r},t) - \nabla\cdot(\kappa(\vec{r})\nabla T(\vec{r},t)) = \frac{H(\vec{r},t)}{\rho c_v}. \quad (2)$$

The heat source density $H(\vec{r},t)$ denotes the thermal energy emitted by a standard volume of material inside the modelled region. Boundary conditions are given by seasonal temperature variations at the seafloor and heat fluxes held zero at vertical boundaries and the geothermal gradient as the lower boundary. A scheme of this model is depicted in Fig. 3.

3.1. Analytic solutions

For demonstrating principal characteristics of sediment temperature evolution from natural sources and power cable thermal impacts, simple analytic solutions of the heat transport equation will be considered and discussed. In particular, this is useful for providing evaluations for the 2 K-criterion in Section 4.2.

3.1.1. Bottom water temperature variations

As noted before, in shallow seas like the Baltic and North Seas bottom sediment temperatures naturally vary with the seasons. The peak-to-peak amplitudes of seasonal temperature variations can be as high as 18 K and their residuals may reach down to a sediment depth of more than 10 m. In order to model this effect, the 1-dimensional heat transfer equation

$$\partial_t T(z,t) - \kappa\partial_z^2 T(z,t) = 0 \quad (3)$$

is solved with temperature $T(z,t)$ as a function of depth (z) and time (t) for a homogeneous sediment with constant thermal diffusivity κ and the annual variation

$$T(z=0,t) = T_{mean} + T_D\cos(\omega t + \varphi) \quad (4)$$

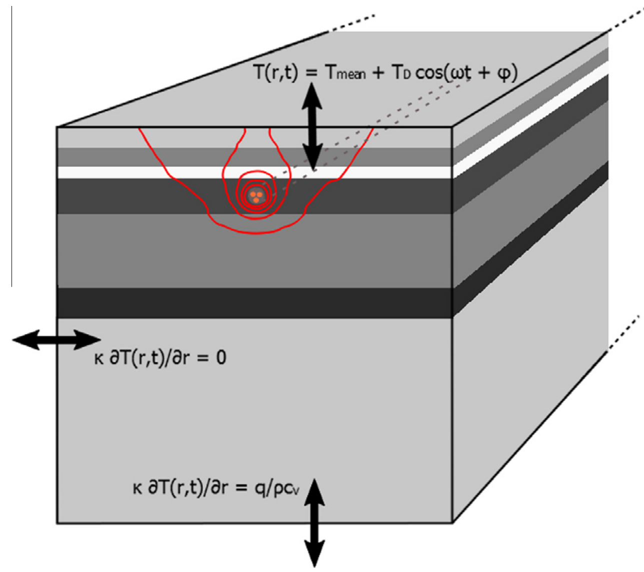

Fig. 3. Sketch showing the 2D model including layered sediment properties, buried cable and boundary conditions.

as a simplified sinusoidal boundary condition at the surface. Since the sediment acts as a low-pass filter, the annual wave is the most efficient and higher orders of temperature variation can be neglected. Here, T_{mean} is the annual mean temperature, T_D the maximum amplitude, ω the annual frequency and φ a phase shift of the annual bottom water temperature variations. The complete solution [20] is as follows

$$T(z,t) = T_{mean} + dT/dz\cdot z + T_D\exp(-\sqrt{\omega/(2\kappa)}z)\cos(\omega t - \sqrt{\omega/(2\kappa)}z + \varphi), \quad (5)$$

where dT/dz is the constant background geothermal gradient (global average $dT/dz = 0.03$ K/m).

3.1.2. Cable as a constant line source

In order to model the cable, a 2-dimensional model is used. For a homogeneous half space, the temperature-depth distribution generated from a continuous line source buried in a depth of z_d with power loss $H(\vec{r},t) = 50\,W/m = const$ is calculated by using the method of mirror images: with $\vec{r} = (x, z - z_d)$ is the vector between the line source and reference point then $\vec{r}_1 = (x, z + z_d)$ is the vector between the mirror image of the line source generated from the solid boundary and the reference point [20]. This assures that the corresponding partial solutions' boundary conditions have zero gradients at the surface. The corresponding analytic solution then can be written as

$$T_{cable}(\vec{r},t) = -\frac{H}{4\pi\kappa}\left[Ei\left(\frac{-\vec{r}^2}{4\kappa t}\right) - Ei\left(\frac{-\vec{r}_1^2}{4\kappa t}\right)\right] \quad (6)$$

with

$$-Ei(-x) = \int_x^\infty \frac{\exp(-u)}{u}du \quad (7)$$

the exponential integral. Since the heat transfer equation is linear, the complete solution including geothermal gradient, bottom-water temperature variations and cable induced heating simply add to

$$T(\vec{r},t) = T_{mean} + dT/dz\cdot z + T_D\exp\left(-\sqrt{\omega/(2\kappa)}z\right)\cos\left(\omega t - \sqrt{\omega/(2\kappa)}z + \varphi\right) + T_{cable}(\vec{r},t). \quad (8)$$

3.2. 2D Finite element modelling (FEM) of a realistic cable in heterogeneous sediment

The FEM model is defined in two dimensions for vertical and horizontal directions as a layered half-space with piecewise constant thermal diffusivities κ and capacities ρc_v. A possible debris deposit originated from cable deployment is ignored, but should be taken into account for future investigations.

The modelling is performed by the finite element method (FEM), using the MATLAB Partial-Differential-Equation-Toolbox [21]. The discretization of the half-space is realized by using a triangular grid refined in the regions of the cable.

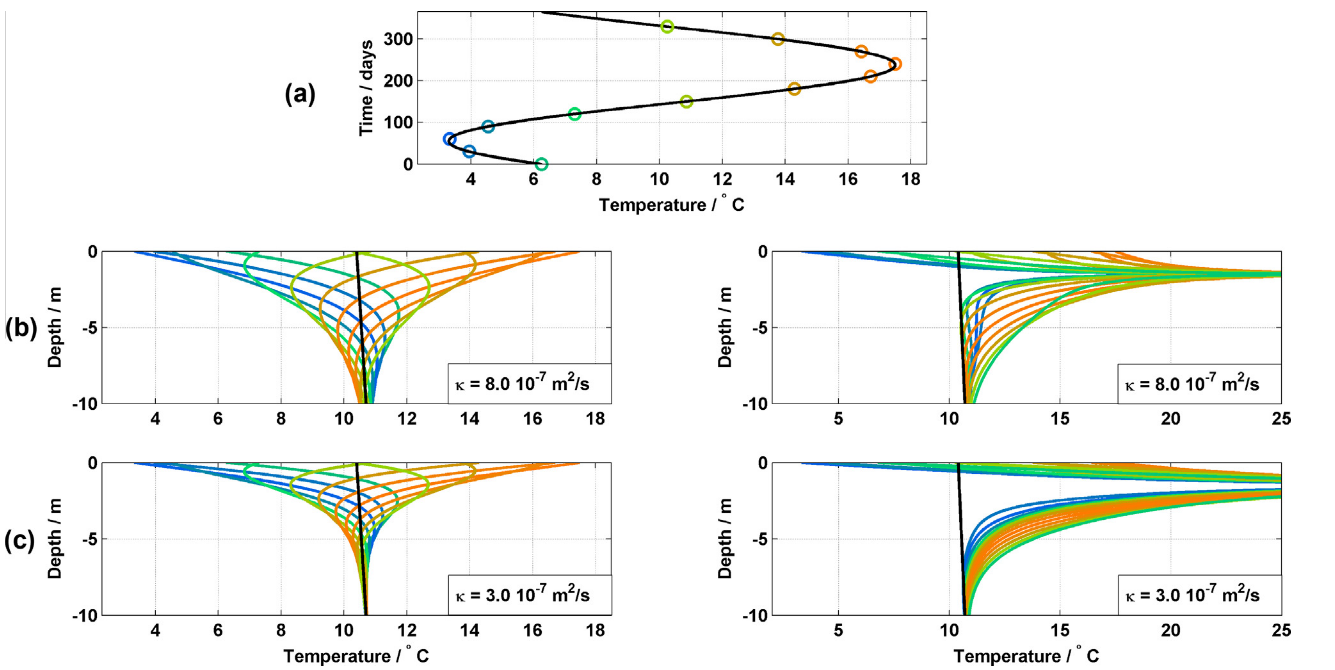

Fig. 4. (**a**) Seasonal bottom water temperature variations approximated by a sinusoidal wave. Analytic solution of the heat transfer equation for (**b**) maximum and (**c**) minimum thermal diffusivities. The resulting temperatures are shown for a scenario with seasonal forcing from the surface only (left) and an additional power cable (constant power loss of 50 W/m and 1.5 m burial depth) (right). Colour code in (**b**) and (**c**) corresponds to the bottom water temperatures in (**a**). (For interpretation of the references to colour in this figure legend, the reader is referred to the web version of this article.)

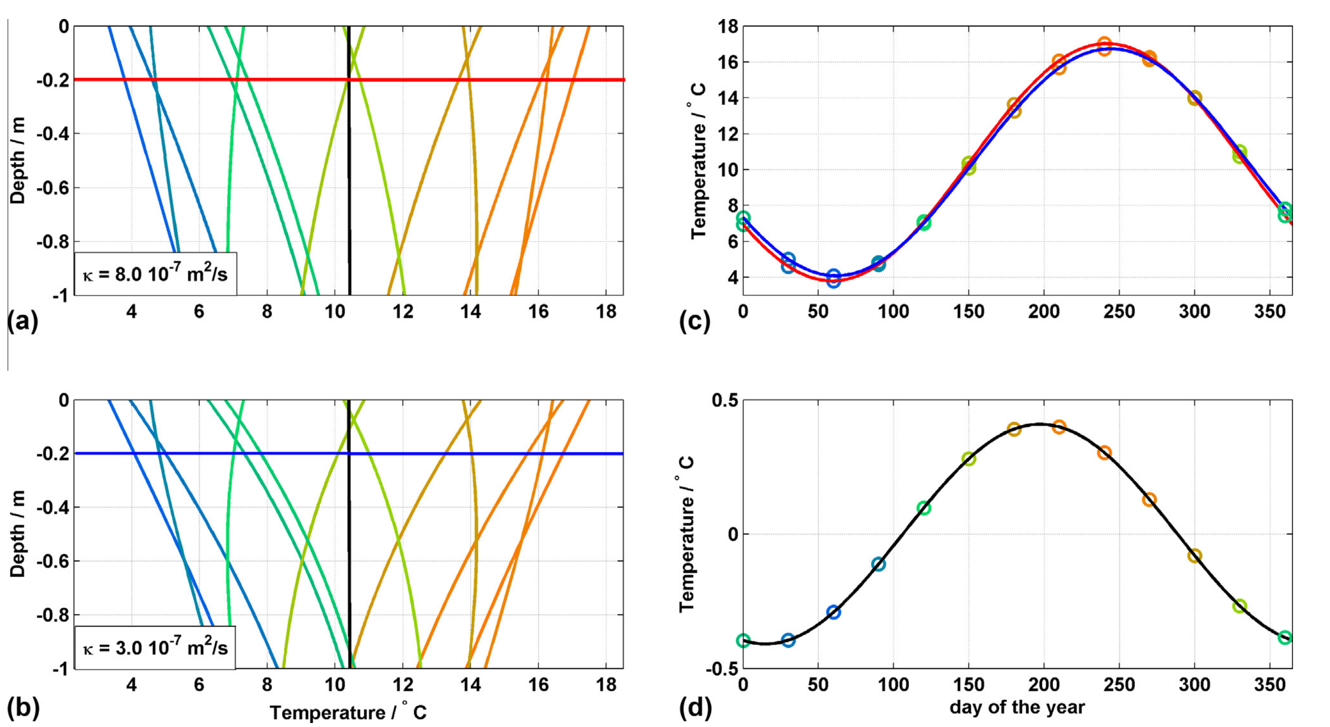

Fig. 5. Temperature-depth profiles resulting from seasonal forcing only for **(a)** maximum and **(b)** minimum thermal diffusivities. Colour coding corresponds to the month as defined in Fig. 4. **(C)** Seasonal temperature in the 2 K depth for high diffusivities (red line from **(a)**) and low diffusivities (blue line from **(b)**). **(d)** Temperature differences from seasonal forcing result in +/0.4 K during the year. (For interpretation of the references to colour in this figure legend, the reader is referred to the web version of this article.)

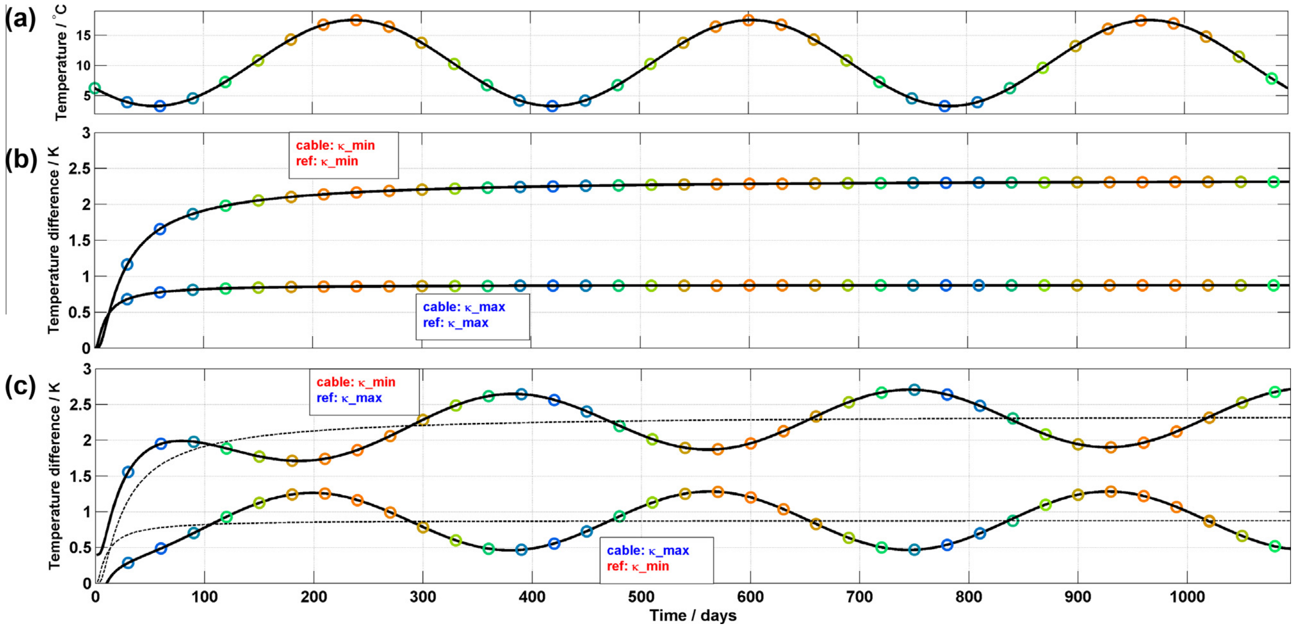

Fig. 6. 2 K differences with a cable in 1.5 m burial depth and a constant power loss of 50 W/m turned on at day 1. The reference point is located 12 m besides the cable. **(a)** 3-year period seasonal bottom water temperature variations. **(b)** 2 K differences for homogeneous sediment, i.e. where the same diffusivities prevail above the cable and the reference point for high and low diffusivities, respectively. **(c)** 2 K differences for heterogeneous sediments, i.e. high diffusivities (κ_max) prevail above the cable but low diffusivities (κ_min) at the reference point and vice versa. Note the oscillation of the temperature differences due to the different penetration velocities and amplitudes of the seasonal signal for both diffusivities. (For interpretation of the references to colour in this figure legend, the reader is referred to the web version of this article.)

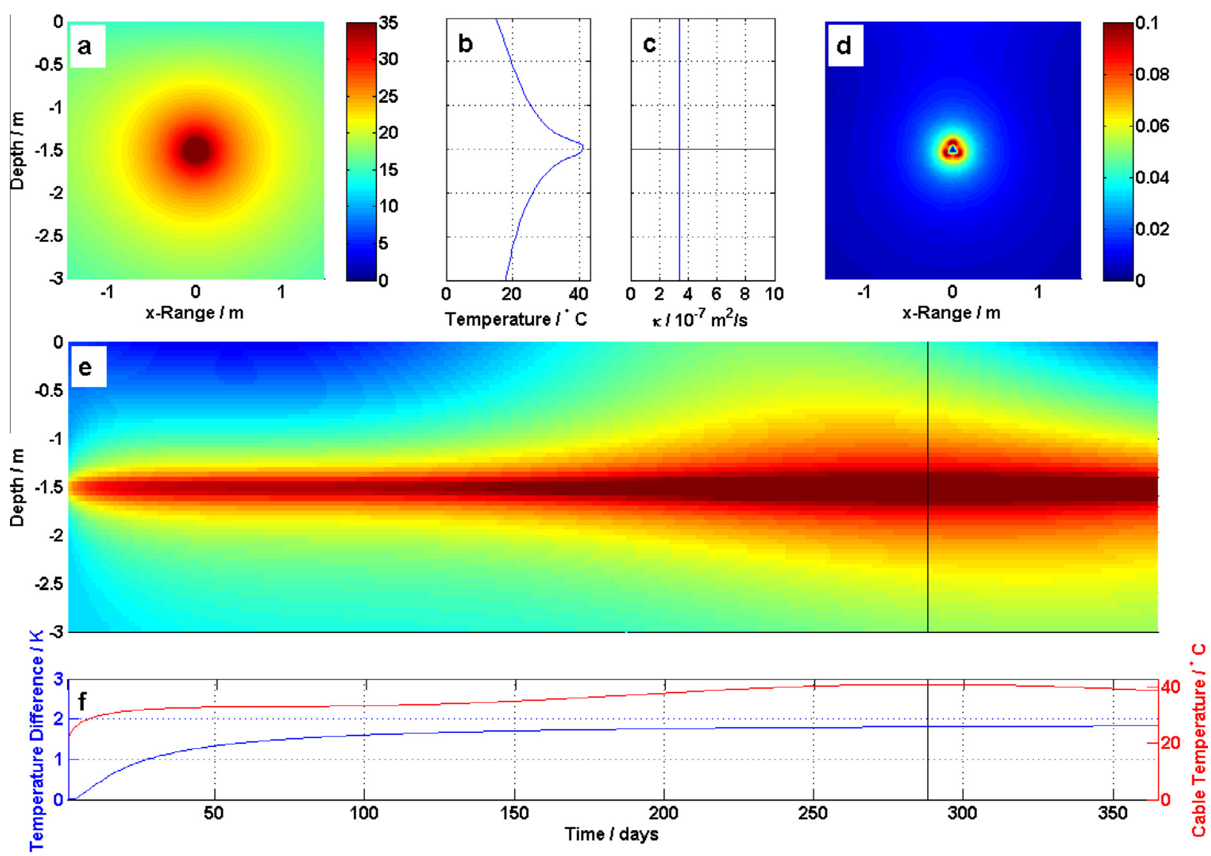

Fig. 7. Temperature evolution for the time frame of one year for up to three meters soil depth with a power cable switched on at day 1 with a constant power loss of 50 W/m. The burial depth of the cable is 1.5 m in a homogeneous thermal diffusivity half space. Sea floor boundary conditions are bottom water temperature variations as defined in 3.1.1: (T_{mean}, T_D, φ) = (10.4 °C, 7.1 °C, 51 days). **(a)** Temperature distribution in and around the cable for the day of the maximum temperature at day 288 with 41.0 °C, and **(b)** temperature-depth profile at day 288. **(c)** Thermal diffusivity-depth profile used as input for the modelling: this follows the conservative assumption of Brakelmann and Stammen [8] with thermal diffusivity $\kappa = 3.4 \cdot 10^{-7}$ m²/s. **(d)** Heat flow in and around the cable. **(e)** Temporal evolution of sediment temperature. **(f)** Maximum cable temperature and 2 K temperature difference over a one year cycle.

As an example, the FEM modelling results for a high voltage alternating current (HVAC) cable are shown, which are widely used for interconnecting offshore wind energy plants and converter platforms of the offshore wind parks. For the thermal parameterizations, a *Submarine Power Cable* 3 × 630 mm², 19/33 (36) kV, Cu [22] was used.

The general setup for the FEM model is:

- Model grid (30 m × 15 m).
- Model resolution with varying mesh size: general 0.3 m, varying and refined at boundaries and inside and around the cable with smallest mesh size of 0.02 m for inside the cable.
- Temporal resolution is 3 h.
- Lower boundary is constrained by the geothermal heat flux as observed by the measurement itself or derived from the literature.
- Upper boundary constrained by seasonal forcing of bottom-water temperatures.
- At the vertical extending boundaries of the region, the flux is set to zero.
- The model was run to steady state with respect to cyclical seasonal forcing using bottom-water temperatures.
- A power cable is set at 1.5 m below the seabed.
- A full year is modelled with a constant power loss of 50 W/m starting at day 1.

Sediment temperatures are calculated for four different scenarios:

Scenario	Description
Conservative	The sediments are assumed to be homogeneous, i.e. use of a constant thermal diffusivity value of $\kappa = 3.4 \cdot 10^{-7}$ m²/s following Brakelmann and Stammen [8]. These thermal properties are used for comparison with measured values for two reasons: first, the work of Brakelmann and Stammen is widely acknowledged in this field of research, and second, because the used thermal properties are solely based on literature values. The new model with thermal diffusivity profiles based on in-situ measurements in the Baltic Sea is compared to a well-studied worst-case model with constant thermal diffusivity based on literature values for water-saturated soils
Deep High	In the 'Deep High' scenario, the thermal diffusivities from Fig. 2a are used, i.e. higher diffusivities in the deeper layers
Top High	In the 'Top High' scenario, the thermal diffusivities from Fig. 2b are used, i.e. higher diffusivities in the upper layers
Overall High	In the 'Overall High' scenario, the thermal diffusivities from Fig. 2c are used, i.e. high diffusivities over the complete depth

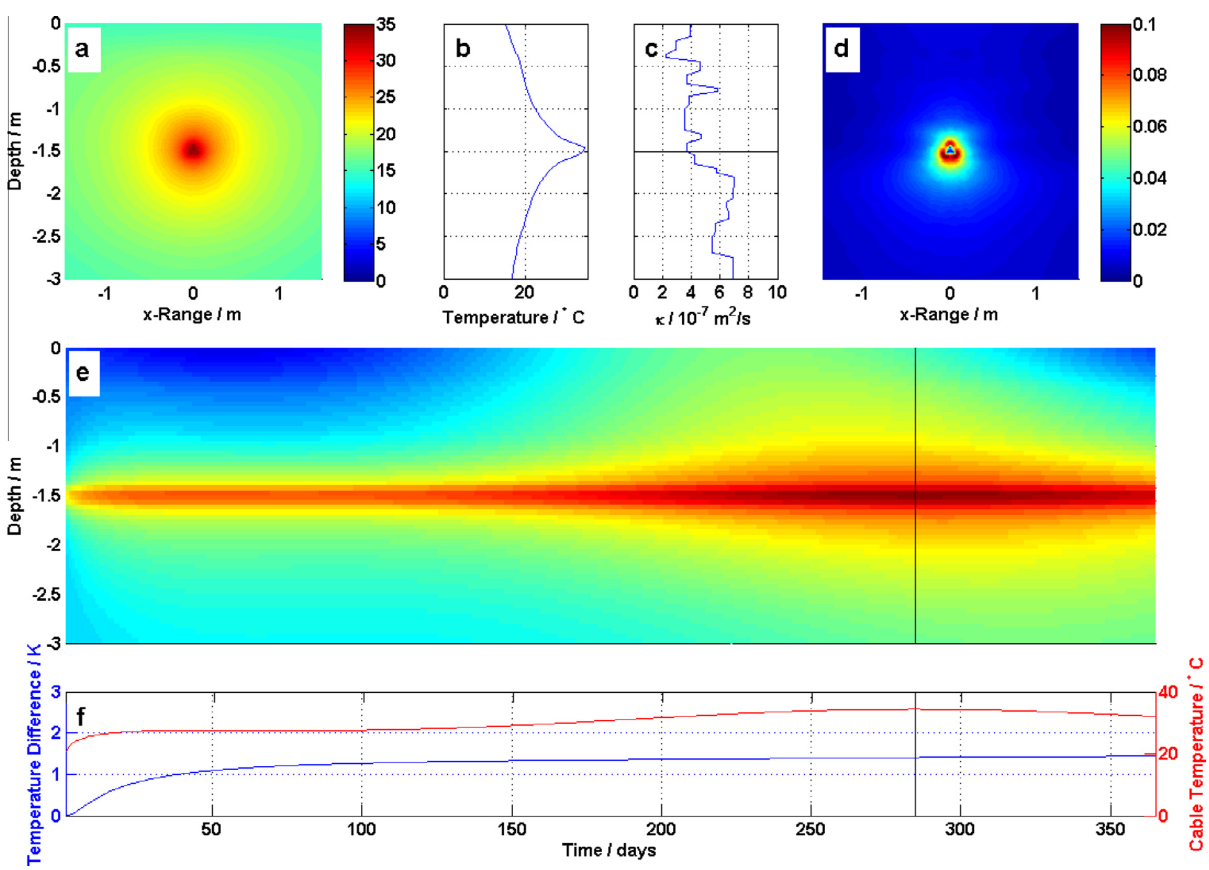

Fig. 8. Same as Fig. 7 but with measured diffusivity profile 'Deep High' (compare Fig. 2). **(a)** Temperature distribution in and around the cable for the day of the maximum temperature at day 285 with 34.3 °C, **(b)** temperature-depth profile for the same day, **(c)** thermal diffusivity-depth profile used as input for the modelling, profile 'Deep High'. **(d)** Heat flow in and around the cable, **(e)** temporal evolution of sediment temperature, **(f)** maximum cable temperature and 2 K temperature difference over a one year cycle.

4. Results

4.1. Analytical 1D-solutions

In this subsection, analytical 1D solutions of the temperature distribution for potential minimum and maximum diffusivities are discussed. These results define the maximum range of temperatures in the sediments over space and time.

For modelling the sediments' temperature field from seasonal bottom-water temperature variations, in Eq. (4) the parameterization (T_{mean}, T_D, φ) = (10.4 °C, 7.1 °C, 51 days) (Fig. 4a) was used as typical values from North Sea observations [3]. This approximation of sinusoidal bottom water temperature variation is justified since this is the strongest seasonal partial wave amplitude; the sediment acting as a low pass filter insensitive to higher frequency variations. The solution (Eq. (5)) shows decreasing amplitudes with depth and an oscillation with depth retarded phase lag (Fig. 4b, showing temperature depth profiles for high ($\kappa = 8.0 \cdot 10^{-7}$ m^2/s) and Fig. 4c for low thermal diffusivities ($\kappa = 3.0 \cdot 10^{-7}$ m^2/s) homogeneous models). The resulting temperature depth profiles incorporating a constant power cable energy loss of 50 W/m according to Eq. (8) again for the high ($\kappa = 8.0 \cdot 10^{-7}$ m^2/s) and low thermal diffusivity ($\kappa = 3.0 \cdot 10^{-7}$ m^2/s) homogeneous models on the right side.

4.2. Reassessment of the 2 K-criterion

The 2 K-criterion was set up by German authorities as a precautionary, conservative benchmark of maximum temperature rise to protect benthic life. Nevertheless, up to now there is no scientific justification for this threshold [23] and no applicable monitoring feasibility. Here, potential biological issues are not discussed. Instead, the strong influence of heterogeneous sediment thermal properties on the evolution of temperature fields will be demonstrated before even a power cable is taken into account. As shown in Section 4.1 different sediments in the North and Baltic Seas yield different temperature depth profiles for low/high thermal conductivities/diffusivities. These heterogeneities provide variability of temperatures in the 2 K depth as high as nearly 1 K without any additional heat from a power cable. These minimum/maximum qualitative estimates were calculated using analytical solutions of the heat transport equation as discussed in Section 3 using homogeneous thermal diffusivity with and without cable.

Simply put, the heterogeneity of the sediments, result in natural variations of the temperature in the 2 K depth. This is demonstrated in Fig. 5 for maximum ($\kappa = 8.0 \cdot 10^{-7}$ m^2/s) and minimum thermal diffusivities ($\kappa = 3.0 \cdot 10^{-7}$ m^2/s). Comparing 0.2 m depth, temperatures at both sites yield temperature differences of about 0.8 K (±0.4 K) during the year from seasonal bottom-water temperature variations. This, of course, might also be exceeded when dealing with even higher or lower diffusivities, which have been measured. Thus, nearly half of the 2 K criterion is already reached without any artificial impact.

The situation changes if a power cable with constant power loss of 50 W/m is incorporated (Fig. 6). The 2 K differences are shown for the "classic" 2 K representation i.e. homogenous sediments with the same maximum or minimum diffusivities above the cable and the reference point (Fig. 6b: asymptotic behaviour with low and high values, respectively). When considering heterogeneous sediments with high diffusivities above the cable and low

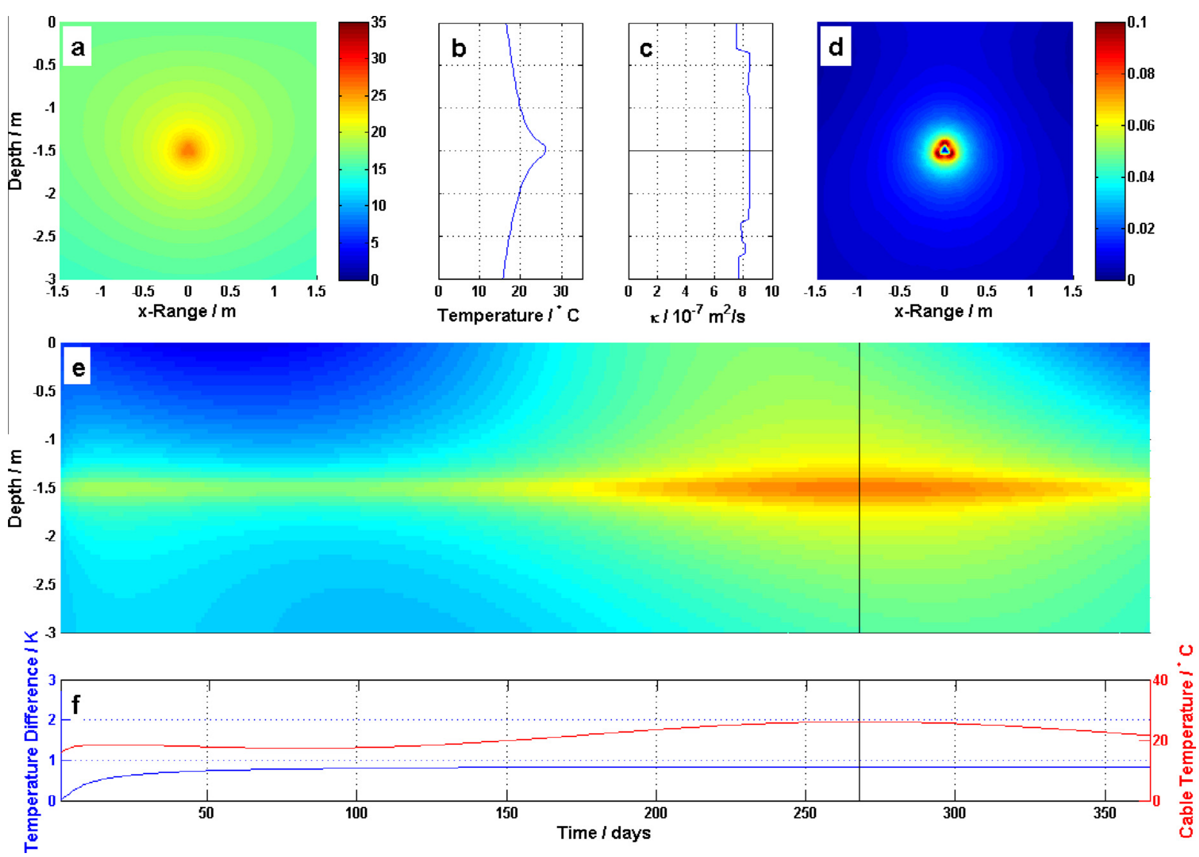

Fig. 9. Same as Fig. 7 but with measured diffusivity profile 'Overall High' (compare Fig. 2). **(a)** Temperature distribution in and around the cable for the day of the maximum temperature at day 268 with 26.0 °C, **(b)** temperature-depth profile for the same day, **(c)** thermal diffusivity-depth profile used as input for the modelling (profile 'Overall High'). **(d)** Heat flow in and around the cable, **(e)** temporal evolution of sediment temperature, **(f)** maximum cable temperature and 2 K temperature difference over one year cycle.

diffusivities at the reference point, the 2 K differences oscillate between 0.5 K and 1.2 K. In the vice versa scenario, high diffusivities at the reference and low diffusivities above the cable, the 2 K differences oscillate between 1.9 K and 2.7 K (Fig. 6c). These differences do not represent the 'true' 2 K differences but are instead apparent values due to the presence of the heterogeneous sediments. Thus, without detailed knowledge of the thermal sediment structure, monitoring and evaluating the 2 K-criterion is unrealistic.

4.3. 2D FEM solutions

By modelling the temperature evolution for realistic thermal properties of the sediments plus including detailed cable thermal properties, maximum thermal stress on the cable itself may be calculated. Thus, by determining maximum cable temperatures for given sediment structure, cable design and/or burial depths can be optimized. Figs. 7–9 show the results for the different scenarios. In each figure, the middle panel **(e)** shows the temporal evolution of sediment temperatures down to a sub-seabed depth of 3 m for 365 days. The power cable is switched on at day 1, i.e. the sediment temperature at day one represents the temperature without additional cable heating.

The upper panels show **(a)** the temperature field around the cable and **(b)** temperature-depth profile, both at the day of maximum cable temperature, **(c)** the thermal diffusivity profile used and **(d)** the heat flux. In **(f)**, the temporal evolution of the maximum cable temperature and the 2 K temperature difference are shown.

Fig. 7 shows the results for the conservative scenario according to Brakelmann and Stammen [8]. The sediments warm during the year because of seasonal heating through the bottom water as well as power loss from the cable, which itself is clearly seen in the high temperatures at 1.5 m depth. Overall temperatures are at maximum (41.0 °C) at day 288 and decrease towards the end of the year due to cooling of the bottom water. The heat flux is maximal around the cable and decreases with distance from the cable. The heat flux is slightly enhanced towards the seabed due to the diffusive cooling through the bottom water. The bottom panel (**f**) shows the temperature of the power cable itself during the year. Also shown is the temperature difference in 0.2 m sediment depth according to the 2 K-criterion, i.e., the temperature in 0.2 m depth minus the temperature without additional heat through power loss. As can be seen, the 2 K-criterion is almost reached towards the end of the year.

Fig. 8 shows the same calculations for the temperature diffusivities for the 'Deep High' scenario. Compared to the conservative scenario, the cable temperature is always about 5–7 K lower and also the temperature at the 2 K depth is lower as a consequence of the overall higher temperature diffusivity. The heat flow around the cable becomes more asymmetrical and there is enhanced lateral heat dissipation in the lower layers.

Fig. 9 shows the effect of higher diffusivity in the upper layers ('Overall High'): The overall temperature of the cable as well as of the surrounding sediments is again lower. This is due to the higher heat fluxes towards the sea floor. The cable temperature now peaks at 26.0 °C in day 268, which is 15 K lower than for the conservative scenario. The temperature in the 2 K depth is again uncritical and settles well below 1 K difference during the whole year.

It can be stated that the temperature distribution crucially depends on the sediment thermal properties. The cable temperature

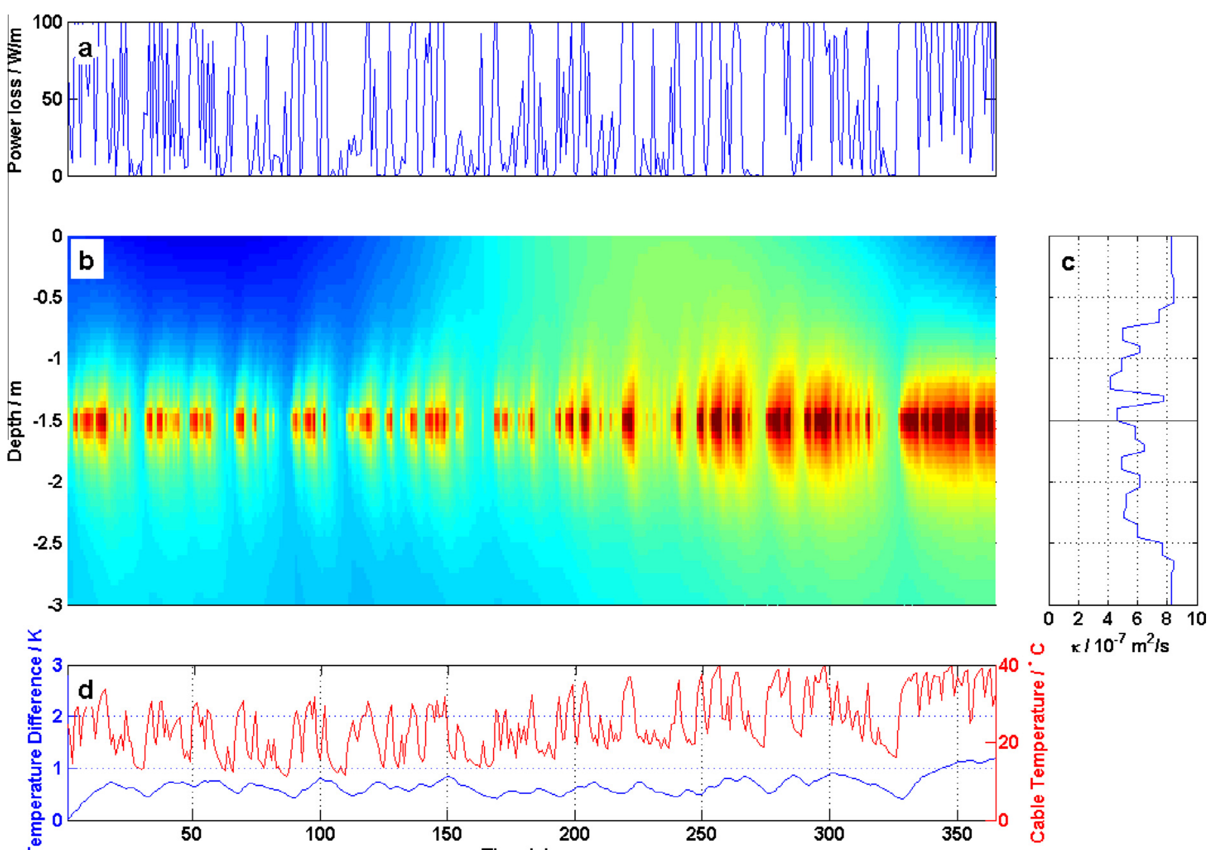

Fig. 10. Profile 'Top High' with realistic power cable loss: **(a)** temporal variation of cable power loss scaled with North Sea FINO1 wind data between 0 and 100 W/m and **(b)** sediment temperatures, **(c)** 'Top High' thermal diffusivity depth profile and **(d)** cable temperature (red) and 2 K temperature difference (blue). (For interpretation of the references to colour in this figure legend, the reader is referred to the web version of this article.)

is almost 10 °C lower in the 'TopHigh' scenario compared to the conservative setting. As a consequence, the temperature difference in the 2 K depth is also much lower. The calculations were made with a constant maximal power loss of 50 W/m during the whole year, which is another worst-case scenario with respect to sediment heating.

Fig. 10 shows the same calculations with a more realistic power loss scenario from wind statistics during the year. Here, the power loss was scaled between 0 and 100 W/m with measured wind data from North Sea FINO1 observing platform using the 'TopHigh' thermal properties. The resulting 2 K temperature difference is well below 1.2 °C during most of the year and maximum cable temperatures of 40 °C.

5. Conclusion

In this paper, it has been shown that the main driving force for the sediment temperature distribution is the seasonal heating and cooling through the sea water strongly modified by the thermal properties of marine sediments. The variabilities as found in the Baltic and North Seas may already account for half of the 2 K-criterion. High voltage cables can be seen as a second order superimposed heat source. Without knowing the distinct thermal properties for a given location, it cannot be derived from the temperature alone whether the power transmission has led to an unduly heating of the upper 20 cm of the sediments. Thus, to verify compliance with monitoring 2 K, a comprehensive, high-resolution state of the sediments thermal state is essential.

To further refine the models, the impact of convective water transport in permeable sediments could be included. At least in the Baltic and North Seas, we have not found any indication of natural, temperature-driven advection in the sediments. If, however, power-transmission would induce pore water advection, this should be regarded in the models. To incorporate advection, the permeability (which is also expected to be highly variable) must be known. In this context, also effects of the alteration of the sediment structure through trenching/burial should be considered.

From a practical point of view, the presented 2D model using in-situ measured sediment properties and prevailing sediment temperatures can be used as a powerful tool with regard to optimizing the burial depths and cable design with respect to both, 'safety' regarding the 2 K-criterion as well as the cable core temperatures.

Acknowledgements

We greatly acknowledge the Norddeutsche Seekabelwerke GmbH for the permission to use the cable specifications and the Baltic Sea thermal parameter data. We want to thank the Bundesministerium für Wirtschaft und Energie (BMWi) and Projektträger Jülich (PTJ) for the permission of using the FINO1 wind data. We thank Lionel Carter for proofreading and three anonymous reviewers for their valuable and constructive reviews. This research did not receive any specific grant from funding agencies in the public, commercial, or non-profit sectors.

References

[1] BSH, Bundesamt für Seeschifffahrt und Hydrographie: Untersuchung der Auswirkungen von Offshore-Windenergieanlagen auf die Meeresumwelt (StUK4), Ergänzung zum Schutzgut Benthos, gemäß StUK4 (BSH 2013) (in German).
[2] BfN, Bundesamt für Naturschutz: Ecological Research on Offshore Wind Farms: International Exchange of Experiences - PART B: Literature Review of the Ecological Impacts of Offshore Wind Farms, BfN-Skripten 186, 2006, 284 pp.
[3] BSH, Bundesamt für Seeschifffahrt und Hydrographie, MARENET monitoring network available at <http://www.bsh.de/de/Meeresdaten/Beobachtungen/MARNET-Messnetz/MARNET.jsp>2013.
[4] J.H. Neher, M.H. McGrath, The calculation or the temperature rise and load capability of cable systems, AIEE Trans. Part III 76 (1957) 752–772.
[5] M.A. Hanna, A.Y. Chikhani, M.M.A. Salama, Thermal analysis of power cables in multi-layered soil. I. Theoretical model, IEEE Trans. Power Delivery 8 (3) (1993) 761–771.
[6] M.A. Hanna, A.Y. Chikhani, M.M.A. Salama, Thermal analysis of power cables in multi-layered soil. II. Practical considerations, IEEE Trans. Power Delivery 8 (3) (1993) 772–778.
[7] C. Garrido, A.F. Otero, J. Cidras, Theoretical model to calculate steady-state and transient ampacity and temperature in buried cables, IEEE Trans. Power Delivery 18 (3) (2003) 667–678.
[8] H. Brakelmann, J.A. Stammen, Thermal Analysis of Submarine Cable Routes: LSM or FEM? in: IEEE Conference Publications, Power and Energy Conference, 2006. PECon '06, pp. 560–565, doi: 10.1109/PECON.2006.346714.
[9] R. de Lieto Vollaro, L. Fontana, A. Vallati, Thermal analysis of underground electrical power cables buried in non-homogeneous soils, Appl. Therm. Eng. 31 (5) (2011) 772–778.
[10] F. De Leon, G.J. Anders, Effects of backfilling on cable ampacity analysed with the finite element method, IEEE Trans. Power Delivery 23 (2) (2008) 537–543.
[11] G.J. Anders, H.S. Radhakrishna, Power cable thermal analysis with consideration of heat and moisture transfer in soil, IEEE Trans. Power Delivery 3 (4) (1988) 1280–1288.
[12] T.J. Hughes, T.J. Henstock, J.A. Pilgrim, J.K. Dix, T.M. Gernon, C.E. Thompson, Effect of sediment properties on the thermal performance of submarine HV cables, IEEE Trans. Power Delivery 30 (6) (2015) 2443–2450.
[13] C.J. Emeana, T.J. Hughes, J.K. Dix, T.M. Gernon, T.J. Henstock, C.E.L. Thompson, J. A. Pilgrim, The thermal regime around buried submarine high voltage cables, Geophys. J. Int. (2016). ggw195.
[14] F. Salata, F. Nardecchia, A. de Lieto Vollaro, F. Gugliermetti, Underground electric cables a correct evaluation of the soil thermal resistance, Appl. Therm. Eng. 78 (2015) 268–277.
[15] G. Evenset, L.E. Klaer, K. Kingman, R. v.d. Thillart, D. Daniela, G.T. de Vries, M. Dillon, Thermal characterization of seabed along the NordLink cable route – results and comparison of measurement methods, CIGRE 2016 Conference Proceedings, 2016 (in press).
[16] R. Hyndman, E. Davis, J. Wright, The measurement of marine geothermal heat flow by a multi penetration probe with digital acoustic telemetry and in-situ thermal conductivity, Mar. Geophys. Res. 4 (1979) 181–205.
[17] M. Dillon, C. Müller, R. Usbeck, Acquiring thermal conductivity data from shear-resistant sediments, Sea Technol. 53 (2) (2012) 57–61.
[18] A. Hartmann, H. Villinger, Inversion of marine heat flow measurements by expansion of the temperature decay function, Geophys. J. Int. 148 (2002) 628–636, http://dx.doi.org/10.1046/j.1365-246X.2002.01600.x.
[19] D.F.C. Pribnow, E.E. Davis, A.T. Fisher, Borehole heat flow along the eastern flank of the Juan de Fuca Ridge, including effects of anisotropy and temperature dependence of thermal conductivity, J. Geophys. Res. 105 (B6) (2000) 13449–13456, http://dx.doi.org/10.1029/2000JB900005.
[20] H.S. Carslaw, J.C. Jaeger, Conduction of Heat in Solids, Oxford University Press, 1959, p. 510.
[21] MathWorks, Partial Differential Equations Toolbox, 2013. <http://www.mathworks.de/products/pde/>.
[22] NSW, Submarine Power Cable $3 \times 630\,mm^2$, 19/33 (36) kV, C, Technical Specification, Medium Voltage Submarine Power Cable, Norddeutsche Seekabelwerke GmbH, 2013.
[23] T. Worzyk, Submarine Power Cables, Springer Verlag, Berlin Heidelberg, 2009, p. 296.